



## H<sub>2</sub> production through the water-gas shift reaction: An *in situ* time-resolved X-ray diffraction investigation of manganese OMS-2 catalyst

Shanthakumar Sithambaram<sup>a</sup>, Wen Wen<sup>c</sup>, Eric Njagi<sup>a</sup>, Xiong-Fei Shen<sup>b</sup>, Jonathan C. Hanson<sup>c</sup>, Steven L. Suib<sup>a,b,\*</sup>

<sup>a</sup> Department of Chemistry, University of Connecticut, U-3060, 55 North Eagleville Rd., Storrs, CT 06269-3060, USA

<sup>b</sup> Department of Chemical, Materials, and Biomolecular Engineering, University of Connecticut, U-3060, 55 North Eagleville Rd., Storrs, CT 06269-3060, USA

<sup>c</sup> Department of Chemistry, Brookhaven National Laboratory, Upton, NY, USA

### ARTICLE INFO

#### Keywords:

Water-gas shift reaction  
*In situ* characterization  
 Manganese  
 Octahedral molecular sieves  
 Hydrogen generation

### ABSTRACT

Manganese oxide octahedral molecular sieve (OMS-2) catalyst prepared by the reflux method was investigated for hydrogen generation via the water-gas shift reaction. Catalysts were characterized using X-ray diffraction (XRD), field emission scanning electron microscopy (FE-SEM), The Brunauer–Emmett–Teller (BET) surface area and determination of average oxidation state (AOS). The OMS-2 catalyst showed very good catalytic activity for the water-gas shift reaction to generate hydrogen under laboratory conditions. An *in situ* study was conducted to monitor the structural changes in the catalyst during the water-gas shift reaction using synchrotron radiation-based time-resolved X-ray diffraction (TR-XRD). During the water-gas shift reaction, the mixed valent OMS-2 catalyst undergoes a structural transformation to form Mn<sub>2</sub>O<sub>3</sub> and finally to form MnO. The study showed that OMS-2 catalysts can be used as inexpensive catalysts for hydrogen generation.

© 2010 Elsevier B.V. All rights reserved.

### 1. Introduction

There is a growing demand for energy around the world and researchers in both industry and academia are striving to develop sustainable energy sources and renewable alternatives to petroleum. Hydrogen has been identified as a very promising renewable clean energy source to satisfy energy needs while protecting the environment. Hydrogen is obtained industrially using the water-gas shift (WGS) reaction, which involves the reaction between carbon monoxide and water to give hydrogen and carbon dioxide as products. ( $\text{CO} + \text{H}_2\text{O} \rightarrow \text{H}_2 + \text{CO}_2$ ). Pt-group metals, such as Au are used as effective catalysts for the WGS reaction because of their high levels of activity and stability [1]. However, Pt- and Au-based catalysts can often display more activity than desired for WGS reactions than Cu-based catalysts [2]. In addition, the noble metals are recognized as a scarce resource as well as a limiting factor in the development of viable energy alternatives to petroleum. Because of the high cost of precious metals, some transition metals with high levels of catalytic activity for the WGS reaction have been evaluated as alternatives. Since the early

1940s the WGS reaction has represented an important step in the industrial production of hydrogen. At the present time, mixtures of Fe–Cr and Zn–Al–Cu oxides are the commercially used catalysts for the water-gas shift reaction at temperatures between 350–500 °C and 180–250 °C, respectively. However, these oxide catalysts are pyrophoric and normally require lengthy and complex activation steps before usage [3]. Therefore, better and inexpensive catalysts are being sought for the generation of hydrogen using WGS reactions [4]. Transition metal oxides have been extensively studied for water-gas shift reactions. Hutchings et al. have studied various mixed manganese oxide catalysts for WGS reactions and found that copper and cobalt manganese oxides are very active at temperatures above 300 °C [5]. In addition, the kinetics of the water-gas shift reaction on manganese oxides under atmospheric pressure have been reported by Krupay et al. [6].

In the recent past, *in situ* spectroscopy in catalysis has gained a lot of attention among scientists because such methods are powerful tools in probing events taking place in a heterogeneous catalyst under reaction conditions. This is crucial for understanding reaction mechanisms of many important chemical processes and would allow the rational design of new or better catalysts [7]. Synchrotron radiation-based *in situ* spectroscopy has become a very powerful method to study catalysts under working conditions. Synchrotron radiation in combination with modern data collection devices makes it possible to conduct sub-minute, time-resolved XRD experiments under a wide variety of temperatures and pres-

\* Corresponding author at: Department of Chemistry, University of Connecticut, U-3060, 55 North Eagleville Rd., Storrs, CT 06269-3060, USA. Tel.: +1 860 486 2797; fax: +1 860 486 2981.

E-mail address: [Steven.Suib@uconn.edu](mailto:Steven.Suib@uconn.edu) (S.L. Suib).

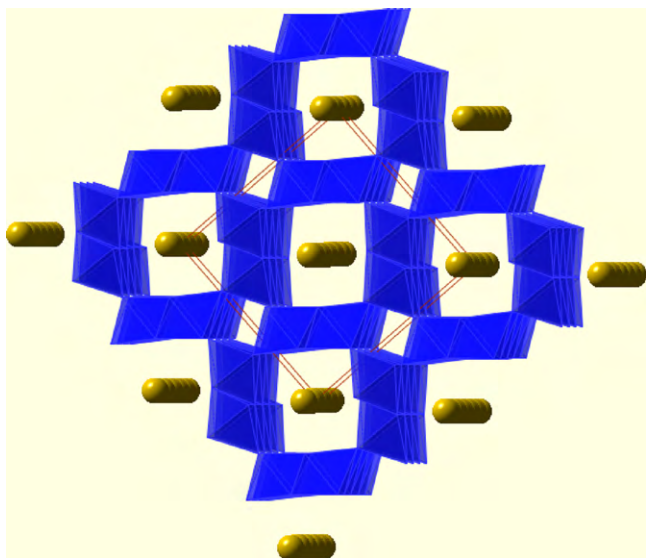


**Fig. 1.** Crystal structure of the OMS-2 catalyst.  $\text{MnO}_6$  octahedra are shown in blue; potassium atoms are shown as brown spheres.

tures [8]. Recently, Shen et al. from our laboratory have successfully used synchrotron X-ray diffraction to study the *in situ* formation of mixed valent manganese oxide nanocrystals [9].

Manganese oxide octahedral molecular sieves (OMS) are well known and these materials have applications in cation-exchange, ion and molecule separation procedures, and chemical sensor, battery, and catalysis applications [10]. OMS-2 catalysts have a  $2 \times 2$  one-dimensional tunnel structure with a pore size of approximately 4.6 Å. Their structures are constructed from edge-shared double chains of  $[\text{MnO}_6]$  octahedra, which are corner-connected to form one-dimensional (1D) tunnel structures (Fig. 1) [11]. Recently, these OMS materials are the subject of intense research as low cost, efficient, and environmentally friendly catalysts [12]. Some of the catalytic applications include the synthesis of imines [13], quinoxalines [14], amino-alcohols [15], epoxides [16], and the oxidation of hydrocarbons [17]. The catalytic activities of the OMS-2 materials vary with their synthesizing methods [18]. In the present study, we describe the use of synchrotron based *in situ* time-resolved X-ray diffraction (TR-XRD) to study the behavior of cryptomelane-type manganese oxide (OMS-2) catalyst under water-gas shift reaction conditions for hydrogen production. The study shows that inexpensive and environmental friendly OMS-2 catalysts can be used to generate hydrogen through the water-gas shift reaction. Further, the structural changes that occur in the catalysts during the reaction process can be monitored using TR-XRD. Optimization of water-gas shift reaction conditions and thorough mechanistic studies is ongoing.

## 2. Experimental

### 2.1. Catalyst preparation

A reflux method described in the literature was employed for the preparation of OMS-2 catalysts [19]. A potassium permanganate solution of 0.4 M and 225 mL was added to a mixture of 67.5 mL of 1.75 M manganese sulfate hydrate solution and 6.8 mL concentrated nitric acid. The dark brown slurry was refluxed in a 500 mL round-bottomed flask with a condenser for 24 h, then filtered and washed with deionized water several times.

### 2.2. Catalyst characterization

#### 2.2.1. XRD

A Scintag Model PDS 2000 diffractometer in a continuous scan mode was used for X-ray powder diffraction (XRD) experiments. Samples were loaded on glass slides, and  $\text{Cu K}\alpha$  radiation [ $\lambda = 1.5418 \text{ \AA}$ ] was used at a beam voltage of 45 kV and 40 mA beam current. The Joint Committee on Powder Diffraction Society (JCPDS) database was used to index the peaks in the XRD patterns.

#### 2.2.2. FE-SEM

A Zeiss DSM 982 Gemini field emission scanning microscope with a Schottky Emitter at an accelerating voltage of 2 kV with a beam current of 1  $\mu\text{A}$  was used to obtain scanning electron micrographs of the OMS-2 catalyst.

#### 2.2.3. BET

The surface area of the OMS-2 catalyst was determined using the Braunauer–Emmet–Teller (BET) method on a Micrometrics ASAP 2010 instrument. Using  $\text{N}_2$  as the adsorbent and a multipoint method the area of OMS-2 was determined.

### 2.3. Average oxidation state

Potentiometric titration was used to measure the average oxidation state (AOS) of the K-OMS-2 catalysts. The catalyst was dissolved in hydrochloric acid so as to convert all the manganese to  $\text{Mn}^{2+}$  and titrated to a  $\text{Mn}^{3+}$  complex with sodium pyrophosphate versus potassium permanganate. This gives total Mn content, based on which the AOS is determined by reducing the solid to  $\text{Mn}^{2+}$  using ferrous ammonium sulfate and back-titrating the excess  $\text{Fe}^{2+}$  with a permanganate standard.

### 2.4. Temperature-programmed reduction

Temperature-programmed reduction (TPR) was carried out by feeding 10%  $\text{H}_2$  in Ar to 25 mg of OMS-2 catalyst in a conventional flow reactor without oxidation treatment prior to measurements. The flow rate of the reducing gas was set at 40 mL/min. The temperature of the reactor was raised from room temperature to 800 °C at a rate of 10 K/min. The rate of  $\text{H}_2$  consumption was determined using a thermal conductivity detector and recorded on an on-line personal computer.

### 2.5. Catalytic experiments

*In situ* time-resolved X-ray diffraction (TR-XRD) experiments were carried out on beam line X7B of the National Synchrotron Light Source (NSLS) at Brookhaven National Laboratory. The experimental set up is similar to that described by Rodriguez et al. [20]. The sample (~1 mg) was loaded into a sapphire capillary cell which was attached to a flow system. A small resistance heater was wrapped around the capillary, and the temperature was monitored with a 0.1 mm chromel–alumel thermocouple that was placed straight into the capillary near the sample. The WGS reaction was carried out isothermally at several temperatures (350, 400, and 500 °C) with a 5% CO and 95% He gas mixture at a flow rate of ~10 mL/min. A heating rate of 3.75 °C/min was used to increase the sample temperature. This gas mixture passed through a water bubbler before entering the reactor. Two dimensional powder patterns were collected with a Mar345 image plate detector and the powder rings were integrated using the FIT2D code. The 3D plots obtained integrating the powder rings of TR-XRD using FIT2D were similar to previous publications from the beamline X7B.

The water-gas shift reaction using OMS-2 catalyst was conducted in our laboratory. Under laboratory conditions, the catalytic

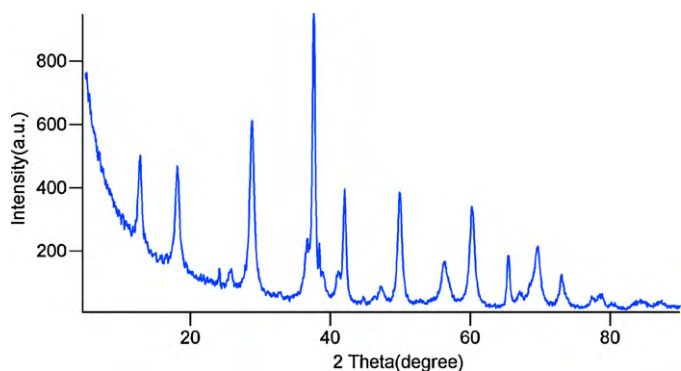


Fig. 2. X-ray diffraction pattern of the OMS-2 catalyst.

activity of OMS-2 was examined in a conventional flow reactor at atmospheric pressure in the temperature range 50–350 °C and at a constant flow rate of 10 mL/min., using 100 mg of catalyst. The gas composition before and after the reaction was analyzed by an on-line gas chromatograph (SRI 8610C, TCD, He (UHP 99.999%, Airgas carrier) with a packed silica gel and molecular sieve column.

### 3. Results

The synthesized OMS-2 catalysts were characterized by XRD, FE-SEM, BET, and average oxidation state determination. The X-ray patterns of the OMS-2 catalysts in Fig. 2 were comparable to that of standard cryptomelane (JCPDS 29-1020) and no other phases were present. An SEM micrograph of OMS-2 catalyst in Fig. 3 shows the typical fibrous morphology of the catalyst. The specific surface area of the OMS-2 sample was determined by the Brunauer–Emmett–Teller (BET) method. The surface area was found to be  $\sim 90 \text{ m}^2 \text{ g}^{-1}$ . Potentiometric titration method to measure the average oxidation state (AOS) revealed that the AOS of the K-OMS-2 catalyst was 3.84.

Time-resolved XRD experimental results are shown in Figs. 4, 7 and 10. The OMS-2 catalyst underwent several structural changes during the water-gas shift reaction as shown in Fig. 4. The final form of the catalyst was MnO, which was consistent with data obtained in comparative experiments in our laboratory (Fig. 9). Fig. 7 shows structural changes of OMS-2 catalyst when  $\text{H}_2$  was passed over the catalyst. The OMS-2 catalyst was reduced to MnO and further reduction to elemental Mn was not observed, which was confirmed by X-ray photoelectron spectroscopy (XPS) studies. When oxygen was passed over the reduced form of the catalyst, the catalyst was oxidized to  $\text{MnO}_2$  as shown in Fig. 10.

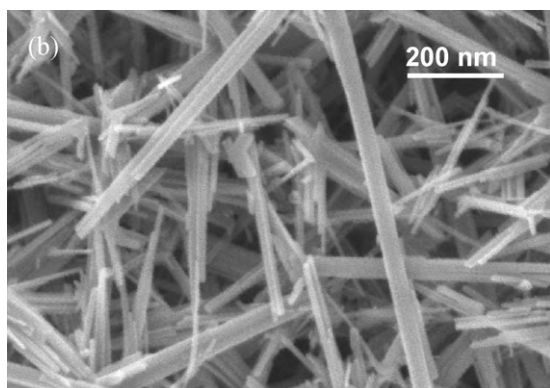


Fig. 3. FE-SEM image of the OMS-2 catalyst.

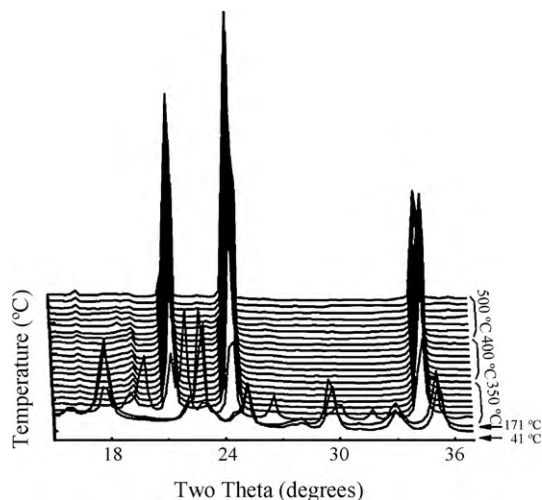
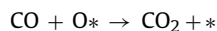
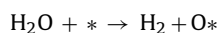


Fig. 4. A 3D plot of *in situ* TR-XRD patterns of OMS-2 catalyst during the water-gas shift reaction. The catalyst was heated from room temperature to 350 °C and WGS reaction was carried out at 350, 400 and 500 °C. XRD patterns were collected continuously with 5 min/pattern ( $\lambda = 0.992 \text{ \AA}$ , beamline X7B, NSLS, BNL).

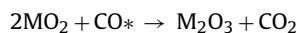
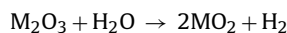
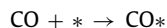
### 4. Discussion

Hydrogen has emerged as an alternative and important source of energy because of its cleanliness. The water-gas shift reaction is widely used in the industrial hydrogen production. This reaction is relatively controllable due to the moderate exothermic nature ( $\Delta H_{298} = -41.1 \text{ kJ/mol}$ ) as opposed to large exothermic heat for the oxidation of CO to  $\text{CO}_2$  ( $\Delta H_{298} = -283 \text{ kJ/mol}$ ). Therefore, the water-gas shift reaction still remains the best means to remove high concentrations of CO from reformed fuels [21]. The kinetics and mechanisms of the WGS reaction with various catalyst systems have been studied in the past by many researchers. Based on kinetic results two types of mechanisms were proposed. The first one is the Rideal–Eley type oxidation–reduction, or regenerative mechanism, in which water oxidizes the surface and CO re-reduces the oxidized surface:

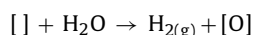
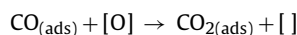


where \* is an active metal site.

The second mechanism describes a bi-functional process where the adsorbed CO on the precious metal or mixed metal oxide is oxidized by the support and then water fills oxygen vacancies of the support [22,23]:



Earlier reports by Krupay et al. kinetic and mechanistic studies with manganese oxides suggest a similar mechanism [6]:



where [O] and [ ] represent an oxygen atom or ion and an oxide vacancy on the surface of the catalyst, respectively. The focus of our present study was to investigate the structural changes that take place on the OMS-2 catalyst during the water-gas shift reaction. The



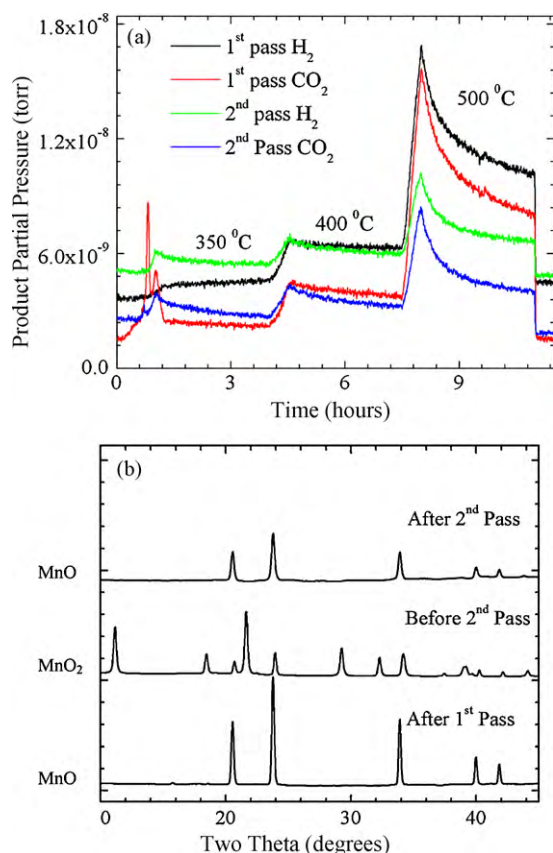


**Fig. 5.** (a) H<sub>2</sub> and CO<sub>2</sub> concentrations measured during the WGS reaction with OMS-2 at various temperatures for 1st and 2nd pass. (b) TR-XRD patterns of OMS-2 catalyst after 1st and before and after 2nd passes.

optimization of reaction parameters, a detailed kinetic and mechanistic study for this OMS-2 catalyzed water-gas shift reaction is underway.

The TR-XRD patterns were collected under water-gas shift (WGS) reaction conditions from room temperature to 350 °C and then holding the temperature at 350, 400 and 500 °C. Fig. 4 shows the structural changes observed on the OMS-2 catalyst during reaction. A sequential reduction of OMS-2 (OMS-2 → Mn<sub>2</sub>O<sub>3</sub> → MnO) occurred during the WGS reaction process. OMS-2 catalyst, which has a cryptomelane structure, transformed to Mn<sub>2</sub>O<sub>3</sub> around 350 °C. Further increases in temperature in the reaction system led to the formation of MnO as the final form of the catalyst. The formation of H<sub>2</sub> during the WGS reaction gradually reduces the mixed valent Mn in the OMS-2 catalyst (average oxidation state ~3.8) to Mn<sup>2+</sup> in MnO. The resulting Mn oxides are nanoparticles with a particle size of ~44 nm. However, these resulting Mn oxides have larger particle size and smaller surface area than that of OMS-2 catalyst.

The concentrations of products of the water-gas shift reaction with OMS-2, H<sub>2</sub> and CO<sub>2</sub>, are shown in Fig. 5a. According to Fig. 5a, the catalytic activity increased with increasing temperature in both the 1st and 2nd pass. However, the catalytic activity in the 2nd pass at 500 °C is less than that in the 1st pass. The structural changes in OMS-2 after the 1st pass due to water-gas shift activity can be attributed to the difference in reactivity. Using the *in situ* experimental set-up at the BNL for this experiment, we were able to detect the products at temperatures only above 300 °C due to the amount of the catalyst used in the micro-reactor. In a separate investigation, OMS-2 catalysts have been found to be active even below 300 °C under laboratory reactor conditions. Fig. 6 shows the results of the water-gas shift reaction activity under laboratory

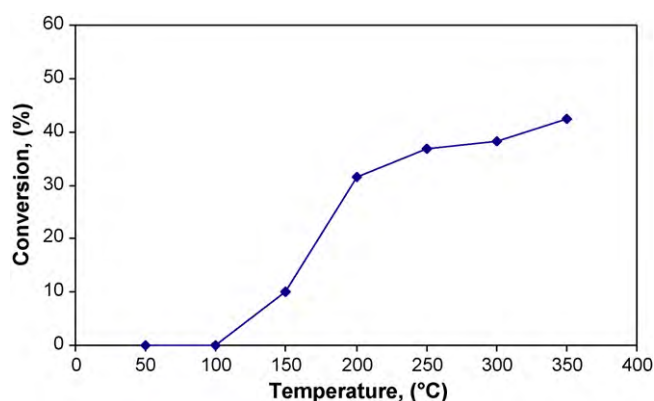


**Fig. 6.** WGS reactivity of OMS-2 catalyst under laboratory conditions. Conversion of CO with temperatures from 50 to 350 °C.

conditions. The activity was monitored at temperatures ranging from 50 to 350 °C. The activity started above 100 °C and continued to increase with increasing temperature. Temperatures below 100 °C are not desirable because water molecules from the reactants are adsorbed on the active sites of the OMS-2 catalyst thus preventing catalytic activity. Furthermore, continuous reaction at 200 °C maintains the structure of OMS-2 for longer period. A faster flow rate has no effect of stability of the catalysts, but decreases the conversion of CO. However, the focus of this paper is to study the structural changes that take place in the catalyst during the WGS reaction using synchrotron radiation. Hence optimal reaction conditions were not used for this study. We are in the process of optimizing WGS reaction conditions with OMS-2 catalysts on a larger lab scale. It will then be feasible to calculate turnover numbers and compare with the performance of the existing systems.

As we described before (Fig. 4), the OMS-2 catalyst is reduced to MnO during the WGS reaction process. However, it is not clear if the reactant carbon monoxide or the product hydrogen induces the reduction of OMS-2 to MnO. CO oxidations with OMS-2 catalysts have been reported previously and the catalysts have been found to be very stable in the presence of CO and oxygen environments. Luo et al. have shown that the activity of OMS-2 for the oxidation of CO is comparable to that found in the Pt/Al<sub>2</sub>O<sub>3</sub> system. They also conducted the reaction with CO in helium (no oxygen) to study the function of lattice oxygen. Pt/Al<sub>2</sub>O<sub>3</sub> system did not show any activity, however, OMS-2 showed the same initial activity and the activity diminished with the consumption of lattice oxygen [24]. To illustrate the role of H<sub>2</sub> in the reduction, a systematic *in situ* reduction of OMS-2 with hydrogen was carried out. H<sub>2</sub> was passed over the OMS-2 catalyst while ramping the temperature from room temperature to 640 °C. TR-XRD were recorded and the results are shown in Fig. 7. Around 400 °C, the diffraction peaks of the OMS-2 catalyst started to disappear and the final diffraction pattern observed corresponded to MnO. This observation is consistent with the TPR experiments conducted with the OMS-2 catalyst. Fig. 8 shows pronounced hydrogen consumption peaks in the temperature range 250–550 °C. The TPR experiment resulted in a greenish powder which was identified as MnO from XRD studies. Furthermore, XRD patterns of the catalyst before and after the water-gas shift reaction under our laboratory conditions are shown in Fig. 9. This further illustrates that the reduced form of the catalyst after the WGS reaction is MnO. In a previous report, Te et al. have studied the structural changes in various manganese oxides (MnO, Mn<sub>3</sub>O<sub>4</sub>, MnO<sub>2</sub>, etc.) feeding carbon monoxide and hydrogen (CO/H<sub>2</sub> = 1:1). Using X-ray diffraction studies on the used catalysts, they have found that these manganese oxides were converted to MnO [25]. This study reveals that MnO is the final form

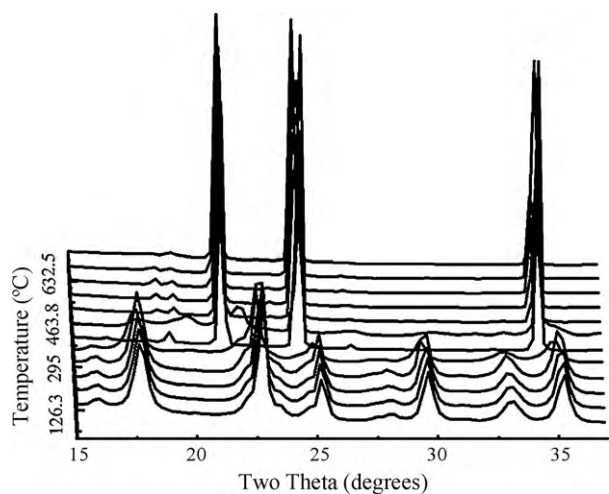


Fig. 7. TR-XRD patterns of the OMS-2 catalyst acquired during the flow of  $H_2$ . The final form of the catalyst observed was MnO.

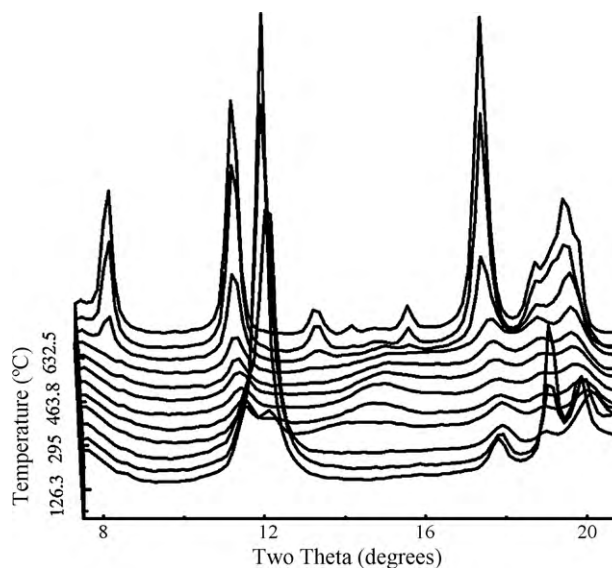


Fig. 10. Time-resolved XRD patterns for the oxidation of reduced MnO catalyst with oxygen.

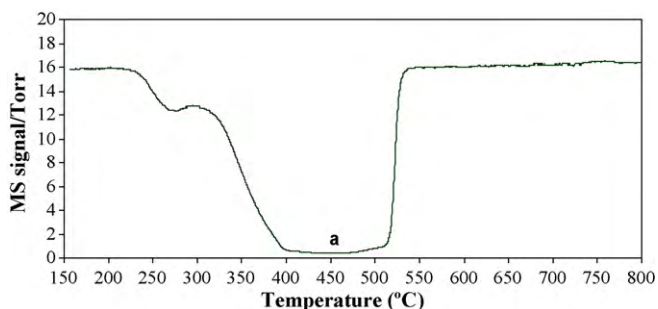


Fig. 8. TPR of OMS-2 catalyst. (a) Reduction of catalyst to MnO.

of the reduced catalyst and further reduction to Mn metal is not possible.

Finally, another experiment was carried out to investigate the structural changes during the reoxidation of the reduced catalyst during the WGS reaction using time-resolved XRD. As we have seen earlier, the OMS-2 catalyst is reduced to MnO in the WGS reaction process. Fig. 10 shows the TR-XRD patterns recorded during the oxidation of MnO in a stream of 5%  $O_2$ /95% He at 300–700 °C. The reoxidation resulted in many phases from  $MnO \rightarrow Mn_3O_4$  and then to  $MnO_2$ . The rapid formation of  $Mn_3O_4$  from MnO is in agree-

ment with reported work by Stobbe et al. [26]. They investigated the utilization of manganese oxide as an oxygen storage compound and reported the various phases observed at different temperatures during the reoxidation of MnO. Their studies showed that the formation of  $Mn_3O_4$  at 673 K and  $Mn_2O_3$  at the same temperature occurred upon prolonged exposure to oxygen. However, they indicated  $MnO_2$  can only be formed at an elevated temperature which was also observed our studies.

## 5. Conclusions

In summary, manganese oxide octahedral molecular sieve catalysts have been used for hydrogen generation using the water-gas shift reaction. OMS-2 catalysts show very good catalytic activity in the water-gas shift reaction above 150 °C. *In situ* TR-XRD shows that the OMS-2 catalyst is transformed to MnO during the WGS reaction. However, the regeneration process of the reduced MnO did not produce OMS-2, but produced an active  $MnO_2$  phase. This investigation essentially reveals the possibility of using an inexpensive tunnel structured manganese oxide material as new catalysts for the water-gas shift reaction to generate hydrogen, which is a significant development in clean energy research.

## Acknowledgements

Authors acknowledge support of the Chemical Sciences, Geosciences and Biosciences Division, Office of Basic Energy Sciences, Office of Science, U. S. Department of Energy. The NSLS is supported by the Divisions of Materials and Chemical Sciences of U.S. Department of Energy. This work was financed by the U.S. Department of Energy, Chemical Sciences Division (DE-AC02-98CH10086). We would also like to thank Dr. Francis Galasso for many helpful discussions. The authors would also like to thank Lei Jin, Thamayanthy Sriskandakumar, and Aimee Morey for their assistance.

## References

- [1] X. Wang, J.A. Rodriguez, J.C. Hanson, D. Gammara, A. Martinez-Arias, M. Fernandez-Garcia, *Top. Catal.* 49 (2008) 81.
- [2] A.A. Phatak, N. Koryabkina, S. Rai, J.L. Ratts, W. Ruettinger, R.J. Farrauto, G.E. Blau, W.N. Delgass, F.H. Ribeiro, *Catal. Today* 123 (2007) 224.
- [3] V. Palma, E. Palo, P. Ciambelli, *Catal. Today* 147S (2009) S107.

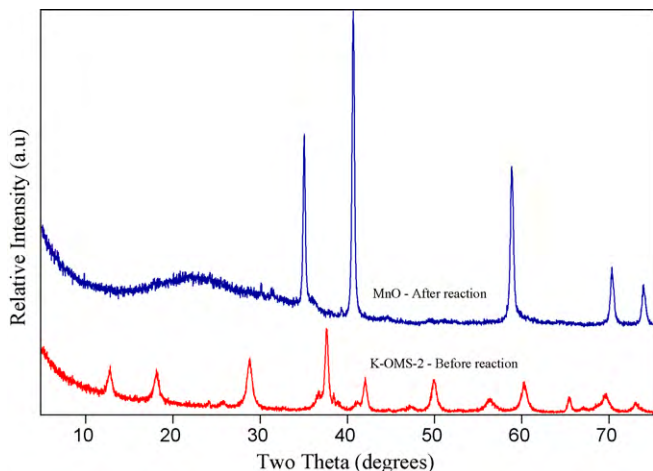


Fig. 9. XRD patterns of catalyst before and after the WGS reaction under laboratory conditions.

- [4] J.A. Rodriguez, P. Liu, J. Hrbek, M. Perez, J. Evans, *J. Mol. Catal. A* 281 (2008) 59.
- [5] (a) G.J. Hutchings, F. Gottschalk, R. Hunter, S.W. Orchard, *Faraday Trans. 1* 85 (1989) 363.
- [6] B.W. Krupay, R.A. Ross, *Can. J. Chem.* 51 (1973) 3520.
- [7] B.M. Weckhuysen, *Chem. Commun.* (2002) 97.
- [8] J.A. Rodriguez, J.Y. Kim, J.C. Hanson, M. Perez, A.I. Frenkel, *Catal. Lett.* 85 (2003) 247.
- [9] X.-F. Shen, Y.-S. Ding, J.C. Hanson, M. Aindow, S.L. Suib, *J. Am. Chem. Soc.* 128 (2006) 4570.
- [10] S.L. Suib, *J. Mater. Chem.* 18 (2008) 1623.
- [11] Y.-S. Ding, X.-F. Shen, S. Sithambaram, S. Gomez, R. Kumar, M.B. Vincent, S.L. Suib, *Chem. Mater.* 17 (2005) 5382.
- [12] K.A. Malinger, Y.-S. Ding, S. Sithambaram, L. Espinal, S. Gomez, S.L. Suib, *J. Catal.* 239 (2006) 290.
- [13] S. Sithambaram, R. Kumar, Y.C. Son, S.L. Suib, *J. Catal.* 253 (2008) 269.
- [14] S. Sithambaram, Y.-S. Ding, W.-N. Li, X.-F. Shen, S.L. Suib, *Green Chem.* 10 (2008) 1029.
- [15] S. Sithambaram, L.-P. Xu, C.-H. Chen, Y.-S. Ding, R. Kumar, C.A. Calvert, S.L. Suib, *Catal. Today* 140 (2009) 162.
- [16] R. Ghosh, X.-F. Shen, J.C. Villegas, Y. Ding, K. Malinger, S.L. Suib, *J. Phys. Chem. B* 110 (2006) 7592.
- [17] S. Sithambaram, E.K. Nyutu, S.L. Suib, *J. Appl. Catal. A* 348 (2008) 214.
- [18] S.L. Suib, *Acc. Chem. Res.* 41 (2008) 479.
- [19] R.N. DeGuzman, Y.-F. Shen, E.J. Neth, S.L. Suib, C.L. O'Young, S. Levine, J.M. Newman, *Chem. Mater.* 6 (1994) 815.
- [20] J.A. Rodriguez, J.C. Hanson, W. Wen, X. Wang, J.L. Brito, A. Matinez-Arias, M. Fernandez-Garcia, *Catal. Today* 145 (2009) 188.
- [21] Y. Tanaka, T. Utaka, R. Kikuchi, T. Takeguchi, K. Sasaki, K. Eguchi, *J. Catal.* 215 (2003) 271.
- [22] J. Barbier Jr., D. Duprez, *Appl. Catal. B: Environ.* 4 (1994) 105.
- [23] Y. Li, Q. Fu, M. Flytzani-Stephanopoulos, *Appl. Catal. B: Environ.* 27 (2000) 179.
- [24] J. Luo, Q. Zhang, J. Garcia-Matinez, S.L. Suib, *J. Am. Chem. Soc.* 130 (2008) 3198.
- [25] M. Te, H.C. Foley, *Appl. Catal. A* 119 (1994) 97.
- [26] E.R. Stobbe, B.A. De Boer, J.W. Geus, *Catal. Today* 47 (1999) 161.